hep-ph/9904378
CERN-TH/99-104

Phenomenological Consequences of Supersymmetry with Anomaly-Induced Masses

Tony Gherghetta, Gian F. Giudice, and James D. Wells

CERN, Theory Division, CH-1211 Geneva 23, Switzerland

Abstract

In the supersymmetric standard model there exist pure gravity contributions to the soft mass parameters which arise via the superconformal anomaly. We consider the low-energy phenomenology with a mass spectrum dominated by the anomaly-induced contributions. In a well-defined minimal model we calculate electroweak symmetry breaking parameters, scalar masses, and the full one-loop splitting of the degenerate Wino states. The most distinctive features are gaugino masses proportional to the corresponding gauge coupling beta-functions, the possibility of a Wino as the lightest supersymmetric particle, mass degeneracy of sleptons, and a very massive gravitino. Unique signatures at high-energy colliders include dilepton and single lepton final states, accompanied by missing energy and displaced vertices. We also point out that this scenario has the cosmological advantage of ameliorating the gravitino problem. Finally, the primordial gravitino decay can produce a relic density of Wino particles close to the critical value.

CERN-TH/99-104
April 1999

1 Introduction

Supersymmetry provides a promising solution to the gauge hierarchy problem afflicting the standard model (SM). However, it is clear that supersymmetry must be broken at low energies. The specific mechanism for transmitting supersymmetry breaking effects is important in determining the low-energy experimental signatures. Currently, there are two known ways that supersymmetry breaking effects appear in the low-energy Lagrangian. In gravity-mediated scenarios [1], supersymmetry is broken in a hidden sector and transmitted gravitationally to the observable sector fields. While this scenario is elegant and simple, it suffers from the supersymmetric flavor problem. Alternatively, in gauge-mediated scenarios [2], supersymmetry breaking is transmitted via gauge forces and this scenario provides an appealing solution to the supersymmetric flavor problem. Both of these alternative scenarios have distinct experimental signatures.

We consider a third scenario for transmitting supersymmetry breaking to the observable sector. In this scenario, rescaling anomalies in the supergravity Lagrangian give rise to soft mass parameters for the observable sector fields [3, 4]. Unlike the gravity-mediated or gauge-mediated scenarios, these anomaly contributions will always be present if supersymmetry is broken. We will refer to the case in which the anomaly-induced masses are dominant as the anomaly-mediated supersymmetry breaking (AMSB) scenario. In this scenario the gaugino mass is proportional to the corresponding gauge beta function while the scalar masses (and A-terms) depend on the anomalous dimensions of the corresponding scalar fields. One of the distinctive features of the AMSB scenario is the gaugino mass spectrum, with the Wino being the lightest supersymmetric particle. Similarly, the squark mass spectrum is unique but unfortunately the slepton mass spectrum is tachyonic. This can be cured by adding a positive, non-anomaly mediated contribution [3]. Some phenomenological consequences of this scenario have been recently presented in ref. [5]. A different and very interesting approach to cure the tachyonic mass spectrum problem has been suggested in ref. [6].

Another distinctive feature of AMSB is that the gravitino is much heavier than the gauginos and squarks. This is cosmologically attractive because the gravitino problem can be ameliorated. Moreover, gravitino decays can produce a present Wino energy density close to the critical value. The neutral Wino is therefore a good dark-matter candidate, in spite

of its negligible thermal relic density.

2 The anomaly-induced mass spectrum

The anomaly-induced soft terms [3, 4] are always present in a broken supergravity theory, regardless of the specific form of the couplings between the hidden and observable sectors. They are linked to the existence of the superconformal anomaly. Indeed they explicitly arise when one tries to eliminate from the relevant Lagrangian the supersymmetry-breaking auxiliary background field by making a suitable Weyl rescaling of the superfields in the observable sector. Their origin has been discussed from various point of views in refs. [3, 4, 6]. Here we give a heuristic derivation of the essential results, and make some comments on their phenomenological relevance.

The effect of supersymmetry breaking can be described by a flat-space chiral superfield Φ, with background value

$$\Phi = 1 - m_{3/2}\theta^2. \tag{1}$$

This field acts as a compensator of the super-Weyl transformation. In other words, by choosing suitable couplings of Φ to the observable fields, the theory is made superconformal invariant.

Let us consider a supersymmetric gauge theory with no mass parameters at the classical level. This does not appear at first sight to be relevant to the minimal supersymmetric model which contains a mass term – the Higgs mixing mass μ – seemingly even in the limit of exact supersymmetry. Actually, the μ term can be viewed as an effect of supersymmetry breaking [7], and therefore we set it to zero for the moment. Mechanisms for generating μ in AMSB scenarios have been discussed in refs. [3, 4, 6]. At the quantum level, there is always the need to introduce a mass parameter, which is the renormalization scale μ (not to be confused with the Higgs mixing parameter). In the presence of a compensator field Φ for super-Weyl transformations, it is natural to expect that the renormalization scale μ is promoted to a superfield, according to

$$\mu \to \mu/\sqrt{\Phi^\dagger \Phi}. \tag{2}$$

The replacement of Φ with its background value given in Eq. (1) generates a specific set of supersymmetry-breaking terms.

The simplest way to obtain the form of the supersymmetry-breaking terms is to employ the technique developed in ref. [8]. The main idea is that when certain parameters of a supersymmetric theory are "analytically continued" into superspace, the renormalization-group (RG) flow of the modified theory is completely determined by the properties of the original theory. In particular, if a parameter is continued into a supersymmetry-breaking background field, the RG properties of the exact supersymmetric theory determine the form of the soft terms. The prescription given in Eq. (2) is a specific example of such a continuation. We can then make use of the general expressions of the gaugino masses M_λ, scalar masses $m_{\tilde{Q}}$, and trilinear couplings A_{Q_i} in terms of derivatives of the field wave-functions [8],

$$M_\lambda = -\frac{1}{2}\left.\frac{\partial \ln S}{\partial \ln \Phi}\right|_0 F_\Phi \tag{3}$$

$$m^2_{\tilde{Q}} = -\left.\frac{\partial^2 \ln Z_Q}{\partial \ln \Phi \partial \ln \Phi^\dagger}\right|_0 F^\dagger_\Phi F_\Phi \tag{4}$$

$$A_{Q_i} = \left.\frac{\partial \ln Z_{Q_i}}{\partial \ln \Phi}\right|_0 F_\Phi. \tag{5}$$

The symbol "$|_0$" denotes setting to zero the Grassmann coordinates, $\theta = \bar{\theta} = 0$. Here S and Z_Q are the gauge and matter field wave-functions, with S related to the gauge coupling constant by $\mathrm{Re}(S)|_0 = g^{-2}/4$. Using Eq. (2) and $F_\Phi = -m_{3/2}$, see Eq. (1), we obtain

$$M_\lambda = -\frac{g^2}{2}\frac{dg^{-2}}{d\ln\mu} m_{3/2} = \frac{\beta_g}{g} m_{3/2} \tag{6}$$

$$m^2_{\tilde{Q}} = -\frac{1}{4}\frac{d^2 \ln Z_Q}{d(\ln\mu)^2} m^2_{3/2} = -\frac{1}{4}\left(\frac{\partial\gamma}{\partial g}\beta_g + \frac{\partial\gamma}{\partial y}\beta_y\right) m^2_{3/2} \tag{7}$$

$$A_y = \frac{1}{2}\sum_i \frac{d\ln Z_{Q_i}}{d\ln\mu} m_{3/2} = -\frac{\beta_y}{y} m_{3/2}. \tag{8}$$

Here the sum $\sum_i$ extends over the fields involved in the Yukawa superpotential term with coupling constant y, and we have used the renormalization group functions $\gamma(g,y) \equiv d\ln Z/d\ln\mu$, $\beta_g(g,y) \equiv dg/d\ln\mu$, and $\beta_y(g,y) \equiv dy/d\ln\mu$.

2.1 Features of the anomaly-induced soft terms

The soft terms in Eqs. (6)–(8) are determined by the anomalous dimensions of the fields or, in other words, by the violation of the Weyl symmetry in the quantum theory given by the conformal anomaly. Indeed, the supergravity prescription in Eq. (2) is sufficient to determine the complete form of the soft terms, by means of the technique of ref. [8].

The form of the soft terms in Eqs. (6)–(8) is particularly interesting because it is invariant under RG transformations. This means that the analytic continuation into superspace given by Eq. (2) defines a consistent RG trajectory for the soft terms. The phenomenological appeal of this form of the soft terms resides precisely in this crucial property. In particular, it entails a large degree of predictivity, since all soft terms can be computed from known low-energy SM parameters and a single mass scale, $m_{3/2}$. Also, it leads to robust predictions, since the RG invariance guarantees complete insensitivity of the soft terms from ultraviolet physics. As demonstrated with specific examples in ref. [4], heavy states do not affect the low-energy parameters in Eqs. (6)–(8), since their effects in the beta-functions and threshold corrections exactly compensate each other. This means that the gaugino mass prediction in Eq. (6) is valid irrespective of the GUT gauge group in which the SM may or may not be embedded. However, exceptions to ultraviolet insensitivity appear in the presence of gauge singlet superfields [6].

The insensitivity from ultraviolet physics not only leads to robust predictivity, but also provides a solution to the supersymmetric flavor problem. Indeed the unknown physics which breaks the flavor symmetry at a high-energy scale Λ_F and determines the Yukawa couplings does not leave any visible trace in the anomaly-mediated soft terms. Recall that in gauge mediation the flavor problem is solved by making the soft terms insensitive to any physics above the messenger scale M. The parameter M is unknown, and is chosen such that $M < \Lambda_F$. The soft terms vanish above the scale M and therefore their low-energy values are finite and have a logarithmic dependence on M. In contrast, in anomaly mediation the soft terms do not vanish at any scale (below the Planck mass M_P), but their values at low energies are not influenced by physics at any intermediate scale.

In order to preserve the attractive properties of the anomaly-mediated soft terms, we have to make sure that other forms of communication of supersymmetry breaking to the

observable sector do not give larger contributions. In ordinary gravity mediation, one makes use of tree-level supersymmetry-breaking communication which, in general, dominates over the loop effects of anomaly mediation. If there are no gauge-singlet superfields with scalar vacuum expectation value of order M_P, then the theory does not contain operators of the form

$$\int d^2\theta \frac{X}{M_P} \mathrm{Tr}\mathcal{W}^\alpha \mathcal{W}_\alpha + \mathrm{h.c.}, \tag{9}$$

where X is the Goldstino superfield. Gaugino masses are only generated by higher-dimensional operators and are at best of order $m_{3/2}^{3/2}/M_P^{1/2}$. In particular, this is in general true in theories with dynamical supersymmetry breaking. In this case, the anomaly-mediated effects give the dominant contributions to gaugino masses [4].

It appears at first difficult to forbid or suppress tree-level gravity contributions to scalar masses, which are obtained by couplings in the Kähler potential between visible sector fields Q and the Goldstino multiplet X,

$$\int d^4\theta \frac{1}{M_P^2} X^\dagger X Q^\dagger Q. \tag{10}$$

However, the suppression is possible if the Kähler potential has the specific structure

$$K = -3M_P^2 \ln(1 - \frac{f_{\mathrm{vis}}}{3M_P^2} - \frac{f_{\mathrm{hid}}}{3M_P^2}), \tag{11}$$

where f_{vis} and f_{hid} are functions of only visible and hidden fields, respectively. This structure could be the result of the underlying fundamental theory such as string theory. However, it is not clear how such a special form of the Kähler potential can be stable against radiative corrections.

A very interesting possibility, pointed out in ref. [3], is that the supersymmetry-breaking and visible sectors reside on different branes embedded into a higher-dimensional space and separated by a sufficiently large distance. In this case, the structure in Eq. (11) is guaranteed by the geometry and not by a symmetry. Thus, all the low-energy soft parameters will arise from anomaly-induced effects.

Unfortunately, it turns out that the pure scalar mass-squared anomaly contribution is negative for the sleptons [3]. In order to avoid this problem we need to consider other positive soft contributions to the spectrum. This can arise in a number of ways, but any of the

solutions will spoil the most attractive feature of anomaly mediation, *i.e.* the RG invariance of the soft terms and the consequent ultraviolet insensitivity. This is, in our opinion, the most disappointing aspect of these scenarios. Nevertheless, there are various options to cure this problem without reintroducing the flavor problem. An example is the inclusion of contributions from fields propagating in the bulk space between the two branes [3]. Another interesting possibility is a combination of gauge- and anomaly-mediated contributions, discussed in ref. [6].

The necessary cure for the slepton masses may completely upset also the mass relations for the other particles (as in the case of the model of ref. [6]). However, here we will simply parametrize the new positive contributions to the scalar squared masses with a common mass parameter m_0, assuming that the extra terms do not reintroduce the supersymmetric flavor problem. We will see that many of the phenomenological features of an anomaly-induced mass spectrum do not crucially depend on the details of the contributions m_0.

2.2 Defining a minimal model

In the AMSB scenario, as discussed above, the necessary mass parameters are the gravitino mass, $m_{3/2}$, and the common scalar mass m_0, which is required to correct the negative mass-squared of the sleptons. The low-energy soft mass spectrum will be

$$M_\lambda = \frac{\beta_g}{g} m_{3/2}, \tag{12}$$

$$m_{\tilde{Q}}^2 = -\frac{1}{4}\left(\frac{\partial\gamma}{\partial g}\beta_g + \frac{\partial\gamma}{\partial y}\beta_y\right) m_{3/2}^2 + m_0^2, \tag{13}$$

$$A_y = -\frac{\beta_y}{y} m_{3/2}. \tag{14}$$

The expressions for the superpartner masses of the minimal particle content and soft parameters are given in the Appendix. We will see that this soft-mass spectrum will give rise to distinctive features which differ from the usual gravity-mediated and gauge-mediated scenarios.

Since our working framework is a theory with anomaly-mediated masses and extra universal contributions to the scalar masses, we operationally construct the full supersymmetric

spectrum from four input parameters,

$$m_{3/2},\, m_0,\, \tan\beta,\, \mathrm{sign}(\mu). \tag{15}$$

We treat the μ and B_μ masses as derived quantities that combine with other terms in the scalar potential to reproduce correct electroweak symmetry breaking (EWSB). This procedure is done with the one-loop effective potential. Also, we assume that Eq. (13) is valid at the GUT scale. As previously discussed, the introduction of the scalar mass m_0 breaks the RG invariance, and therefore we must define a scale for the boundary condition Eq. (13). Notice, however, that at the one-loop level with Yukawa couplings neglected, the squark and slepton squared masses are renormalized additively. Therefore, in this case, we do not need to specify at which scale Eq. (13) is valid. However this is not true, for instance, for the stop and Higgs mass parameters.

We find that electroweak symmetry breaking can be accommodated with the above framework. Successful EWSB correlates with values of $|\mu|$ typically between 3 to 6 times the Wino mass as long as m_0 is not significantly higher than the anomaly-mediated contributions to the squark masses. Otherwise, $|\mu|$ can be larger. The relative size of μ with respect to M_2 becomes important when considering mass splitting among the degenerate Wino triplet states. This will be considered in more detail in the next section.

In Fig. 1 we demonstrate a subset of superpartner masses using a generically chosen set of input parameters, $m_{3/2} = 36\,\mathrm{TeV}$, $\tan\beta = 5$, and $\mu < 0$. The choice of $m_{3/2} = 36\,\mathrm{TeV}$ determines the gaugino masses to be $M_1 = 333\,\mathrm{GeV}$, $M_2 = 119\,\mathrm{GeV}$, and $M_3 = 850\,\mathrm{GeV}$. We vary m_0 to demonstrate its dependence in the scalar mass spectrum. The squark masses are rather insensitive to values of m_0 that raise the slepton masses above their anomaly-mediated tachyonic values. The sleptons, $\tilde{e}_L$ and $\tilde{e}_R$, are nearly equal in mass. The extraordinary degeneracy of these slepton masses will be expounded upon in the following section.

In Fig. 1 we also plot the lightest physical Higgs boson mass, m_h. This is roughly constant over the range of m_0, since this eigenvalue admits only logarithmic sensitivity to supersymmetry breaking scales. Requiring $M_2 > 90\,\mathrm{GeV}$ and assuming $\tan\beta > 1.8$ (for perturbative unification at the GUT scale), we find a lower bound on the lightest scalar Higgs boson mass of 70 GeV. The lower bound exceeds 100 GeV for $\tan\beta > 5$. The upper bound on the Higgs boson mass, assuming $M_2 < 500\,\mathrm{GeV}$ and $m_0 < m_{\tilde{q}}$ is 125 GeV. However,

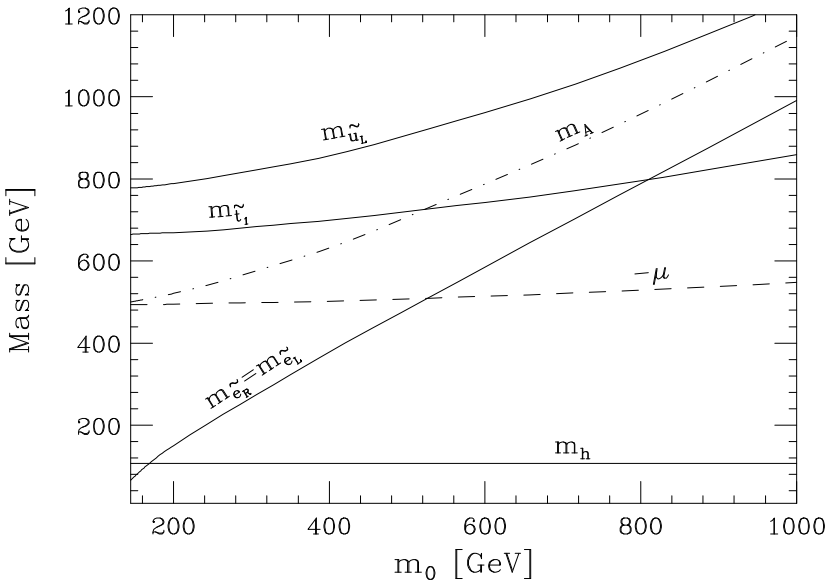

Figure 1: Masses of several states in the supersymmetric spectrum as a function of m_0 with $m_{3/2} = 36\,\text{TeV}$, $\tan\beta = 5$, and $\mu < 0$. The gaugino masses for this choice are $M_1 = 333\,\text{GeV}$, $M_2 = 119\,\text{GeV}$, and $M_3 = 850\,\text{GeV}$.

the squark masses are above 3 TeV when the bound is saturated. Since such high squark masses are not welcome in the loop-corrected Higgs potential, the Higgs mass is expected to be lighter than 125 GeV in AMSB. On the other hand, the pseudoscalar Higgs mass, m_A, depends linearly on the supersymmetry breaking scale, and therefore increases with m_0 as shown in the figure. In the next section, we study a few of the unique features of the AMSB spectrum, and how it impacts search capabilities at high-energy colliders.

3 Phenomenology

A unique feature of anomaly-mediated supersymmetry is the gaugino mass hierarchy. To compute the gaugino masses we include next-to-leading corrections coming from α_s and $\alpha_t \equiv y_t^2/4\pi$ two-loop contributions to the beta-functions and weak threshold corrections enhanced by a logarithm. In this approximation, we find

$$M_1^{NLO} \;=\; M_1(Q)\left\{1 + \frac{\alpha}{8\pi\cos^2\theta_W}\left[-21\ln\frac{Q^2}{M_1^2} + 11\ln\frac{m_{\tilde{q}}^2}{M_1^2} + 9\ln\frac{m_{\tilde{\ell}}^2}{M_1^2}\right.\right.$$

$$+ \quad \ln\frac{\mu^2}{M_1^2} + \frac{2\mu}{M_1}\sin 2\beta \frac{m_A^2}{\mu^2 - m_A^2}\ln\frac{\mu^2}{m_A^2}\Bigg] + \frac{2\alpha_s}{3\pi} - \frac{13\alpha_t}{66\pi}\Bigg\} \tag{16}$$

$$M_1(Q) = \frac{11\alpha(Q)}{4\pi\cos^2\theta_W} m_{3/2} \tag{17}$$

$$M_2^{NLO} = M_2(Q)\Bigg\{1 + \frac{\alpha}{8\pi\sin^2\theta_W}\Bigg[-13\ln\frac{Q^2}{M_2^2} + 9\ln\frac{m_{\tilde{q}}^2}{M_2^2} + 3\ln\frac{m_{\tilde{\ell}}^2}{M_2^2}$$

$$+ \quad \ln\frac{\mu^2}{M_2^2} + \frac{2\mu}{M_2}\sin 2\beta \frac{m_A^2}{\mu^2 - m_A^2}\ln\frac{\mu^2}{m_A^2}\Bigg] + \frac{6\alpha_s}{\pi} - \frac{3\alpha_t}{2\pi}\Bigg\} \tag{18}$$

$$M_2(Q) = \frac{\alpha(Q)}{4\pi\sin^2\theta_W} m_{3/2} \tag{19}$$

$$M_3^{NLO} = M_3(Q)\left\{1 + \frac{3\alpha_s}{4\pi}\left[\ln\frac{Q^2}{M_3^2} + F\left(\frac{m_{\tilde{q}}^2}{M_3^2}\right) - \frac{14}{9}\right] + \frac{\alpha_t}{3\pi}\right\} \tag{20}$$

$$F(x) = 1 + 2x + 2x(2-x)\ln x + 2(1-x)^2\ln|1-x| \tag{21}$$

$$M_3(Q) = -\frac{3\alpha_s(Q)}{4\pi} m_{3/2}. \tag{22}$$

The higgsino corrections to M_1 and M_2 are proportional to $\mu/M_{1,2}$ and can become very important in models with large μ, as discussed in ref. [4]. The NLO corrections are significant, especially for M_2 where the $6\alpha_s/\pi$ contribution changes the Wino mass by more than 20%.

The mass ratios of the gauginos M_1:M_2:$|M_3|$ are approximately $3.3 : 1 : 8.8$ at leading order. At NLO, these ratios are changed to $2.8 : 1 : 7.1$. This implies that a nearly degenerate triplet of Winos ($\tilde{W}^{\pm}$, $\tilde{W}^0$) are the lightest gauginos. We shall see below that the neutral $\tilde{W}^0$ is the lightest in the triplet, and is a candidate lightest supersymmetric partner (LSP). In an R-parity conserving theory the $\tilde{W}^0$ is stable and escapes detection at a high-energy collider. Therefore, visible particles produced in association with the $\tilde{W}^0$ states will be required to uncover evidence of supersymmetry.

It is also possible that the LSP is a sneutrino. This would be the case if the additional contributions to the scalar masses were large enough to generate a positive mass-squared for the sleptons but still smaller than the Wino mass. In this case, Wino decays would generally produce leptons and sneutrinos in the final state. We will consider this possibility in some detail in sect. 3.4.

3.1 Mass splitting among Winos

The first step in considering light Wino states is to calculate the mass splitting between the charged and neutral states. For the moment we shall ignore loop corrections and describe the tree-level splitting that develops for light Wino states. Upon integrating out the heavy Bino and Higgsino states, we are left with an effective theory with several operators that could shift the mass of the remaining chargino and neutralino states to be different than M_2. Operators of the form $\mathcal{O} = M_{ab}\tilde{W}^a\tilde{W}^b$ will generate mass splittings for the Winos only if M_{ab} transforms non-trivially under $SU(2)$. Because of the symmetry property of the Majorana mass term, M_{ab} must have isospin 2, and the lowest-dimensional operator which generates a mass splitting is

$$\mathcal{O} = \frac{1}{\Lambda^3}(H^\dagger\tau^a H)\,(H^\dagger\tau^b H)\,\tilde{W}^a\tilde{W}^b, \tag{23}$$

where $\Lambda \sim M_1, \mu$ and H denote the Higgs doublets. Therefore, we see from the above that all mass splittings at tree-level must occur with m_W^4/Λ^3 suppression.

A more detailed formula for the tree-level mass splitting[†] with $|\mu| \gg M_1, M_2, m_W$ is[‡]

$$\begin{aligned} m_{\tilde{\chi}_1^\pm} - m_{\tilde{\chi}_1^0} \;=\; & \frac{m_W^4 \sin^2 2\beta}{(M_1 - M_2)\mu^2}\tan^2\theta_W + 2\frac{m_W^4 M_2 \sin 2\beta}{(M_1 - M_2)\mu^3}\tan^2\theta_W \\ & + \frac{m_W^6 \sin^3 2\beta}{(M_1 - M_2)^2\mu^3}\tan^2\theta_W(\tan^2\theta_W - 1) + \mathcal{O}(\frac{1}{\mu^4}). \end{aligned} \tag{24}$$

When this formula is valid and μ is determined by the electroweak-breaking condition, the mass splitting is negligible compared to the charged pion mass – an important mass scale for the phenomenology of Wino decays. In our numerical analysis, we will always calculate the chargino and neutralino mass splittings from the exact formula and not from the expansion in Eq. (24), given here only for illustrative purposes. Notice also that, in the large $\tan\beta$

[†]To generate a Wino mass splitting, it is also necessary to break the global custodial $SU(2)_V$ defined such that the matrix $\Phi = \begin{pmatrix} H_d^0 & H_u^+ \\ H_d^- & H_u^0 \end{pmatrix}$, constructed from the two Higgs doublets, transforms as $\Phi \to V\Phi V^\dagger$ with V unitary. The μ term is invariant, since it can be written as $\mu\,\mathrm{det}\Phi$. The symmetry is preserved by electroweak breaking, as long as $\tan\beta = 1$, but it is broken by hypercharge effects. Therefore Eq. (24) has to vanish in the limit $\tan\beta \to 1$ and $\tan\theta_W \to 0$.

[‡]Our sign convention for μ is set by $W = \mu(H_u^0 H_d^0 - H_u^+ H_d^-)$.

limit, the Wino mass difference becomes

$$m_{\tilde{\chi}_1^\pm} - m_{\tilde{\chi}_1^0} = \frac{M_2 m_W^4}{2\mu^4}\left(1 + \frac{2M_2 \tan^2\theta_W}{M_1 - M_2}\right) + \mathcal{O}(\frac{1}{\mu^6}), \quad \text{for } \tan\beta \to \infty. \tag{25}$$

In this limit the mass difference has a further suppression factor, M_2/μ because the necessary chiral flip cannot originate from the Higgsino mass.

The dominant contribution to the Wino mass splitting does not come from the tree-level result described above, but rather due to one-loop corrections in the chargino and neutralino mass matrices. We have done a full numerical calculation of the one-loop corrected chargino and neutralino mass matrices using the formulae of ref. [9]. For the anomaly-mediated spectrum, with only positive mass-squared additional contributions to all the scalar masses, we find that the gauge-boson loop corrections dominate the mass splitting. This is because in the typical anomaly-induced mass spectrum the squark masses are heavy and the μ parameter is large. Consequently, following the argument that led us to Eq. (23), we infer that their contribution to the Wino mass splitting is suppressed by M_W^4/Λ^3. On the other hand, the effect of gauge-boson loops cannot be described by local operators. Isolating this contribution in the limit of large μ, we find (see also refs. [11, 5])

$$\Delta_\chi \equiv m_{\tilde{\chi}_1^\pm} - m_{\tilde{\chi}_1^0} = \frac{\alpha M_2}{\pi \sin^2\theta_W}\left[f(m_W^2/M_2^2) - \cos^2\theta_W f(m_Z^2/M_2^2)\right] \tag{26}$$

where

$$f(x) \equiv -\frac{x}{4} + \frac{x^2}{8}\ln x + \frac{1}{2}(1+\frac{x}{2})\sqrt{4x-x^2}\left[\arctan\frac{2-x}{\sqrt{4x-x^2}} - \arctan\frac{x}{\sqrt{4x-x^2}}\right]. \tag{27}$$

In the limit that $M_2 \to \infty$, the expression in Eq. (26) simply becomes

$$\Delta_\chi = \frac{\alpha\, m_W}{2(1+\cos\theta_W)}\left[1 - \frac{3}{8\cos\theta_W}\frac{m_W^2}{M_2^2} + \mathcal{O}\left(\frac{m_W^3}{M_2^3}\right)\right], \tag{28}$$

which has the asymptotic limit $\Delta_\chi = \alpha\, m_W/[2(1+\cos\theta_W)] \simeq 165$ MeV.

It may appear odd that the mass splitting should asymptote to a constant value as M_2 gets arbitrarily massive. This behavior can be understood in momentum space as an infrared mismatch between the self-energies of $\tilde{W}^+$ and $\tilde{W}^0$ regulated by m_W. Or, equivalently, since $SU(2)$ is a good theory for short distances $r \ll m_W^{-1}$, we can calculate the Coulomb energy

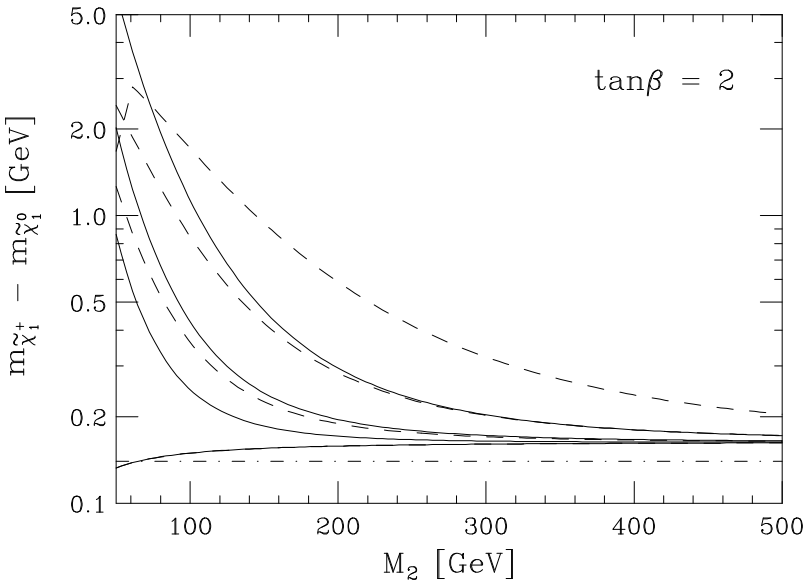

Figure 2: The mass splitting as a function of M_2 for $\tan\beta = 2$. The solid curves, from top to bottom, represent $\mu = 2M_2$, $\mu = 3M_2$, $\mu = 5M_2$, and $\mu = \infty$. The dashed curves are the same except for the opposite sign of μ. The dot-dashed curve is the charged pion mass $m_{\pi^\pm}$.

of the charged state for large distances $r \gtrsim m_W^{-1}$ (infrared region) to obtain a mass splitting of approximately αm_W. The exact prefactors are given in Eq. (28).

In Figs. 2 and 3 we show the total calculated mass splitting as a function of M_2 for $\tan\beta = 2$ and 10. In our numerical calculation, we include the full one-loop result and we do not use the approximate expressions given in Eq. (26). The solid curves, from top to bottom, represent $\mu = 2M_2$, $\mu = 3M_2$, $\mu = 5M_2$, and $\mu = \infty$. The dashed curves are the same except that $\mu < 0$. The dot-dashed curve is the charged pion mass $m_{\pi^\pm}$. As $\tan\beta$ increases the sign of μ becomes less and less relevant in the calculation of the mass splitting. When $\tan\beta = 40$ the solid and dashed curves are irresolvable.

In an anomaly-mediated spectrum with radiative electroweak symmetry breaking, the typical relation between M_2 and μ is $3 \lesssim |\mu|/M_2 \lesssim 6$. This is true as long as the squark masses are not increased significantly beyond their anomaly-mediated baseline values from the universal mass contributions that lift the slepton mass-squared to positive values. This is also acceptable from naive fine-tuning arguments. Larger values of μ lead to an unnatural Higgs potential. For $|\mu|/M_2 = 5$ we find from Figs. 2 and 3 that the mass splitting is

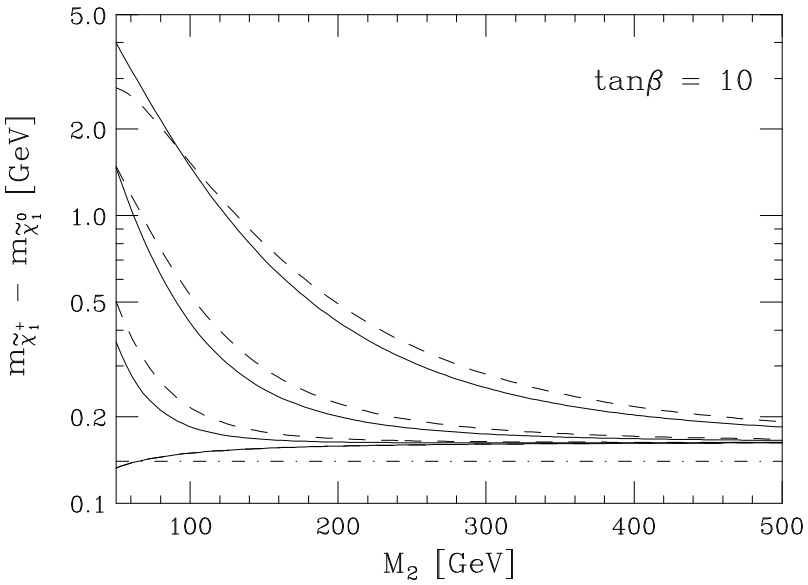

Figure 3: The mass splitting as a function of M_2 for $\tan\beta = 10$. The solid curves, from top to bottom, represent $\mu = 2M_2$, $\mu = 3M_2$, $\mu = 5M_2$, and $\mu = \infty$. The dashed curves are the same except for the opposite sign of μ. The dot-dashed curve is the charged pion mass $m_{\pi^\pm}$.

significantly above $m_{\pi^\pm}$ such that $\tilde{W}^\pm \to \tilde{W}^0\pi^\pm$ is kinematically allowed and is the dominant decay mode. This remark is also true even for extraordinarily large values of μ as long as $M_2 \gtrsim 80\,\text{GeV}$.

3.2 Finding supersymmetry with dileptons

The precise calculation of the mass splitting is crucial since in ref. [10] it was demonstrated that if $m_{\pi^\pm} \lesssim m_{\tilde{\chi}_1^\pm} - m_{\tilde{\chi}_1^0} \lesssim 1\,\text{GeV}$ then the $\tilde{W}^\pm$ will decay too fast to use a quasi-stable charged particle analysis, with dedicated triggers. However, the decays are not prompt, and so analyses of events triggered by other means could see a stiff charged particle track that subsequently terminates in the vertex detector. The difficulty is triggering the event.

One way to trigger such events is to produce the Winos in associated production with a standard model particle, such as a gluon at hadron colliders or a photon at e^+e^- colliders. Triggering on high-p_T monojets or high-energy photons at these colliders then may be an effective way to trigger the events and save them for future analysis [10, 12, 5]. At the

analysis stage a kink in the vertex detector, or a terminating stiff track, would then indicate a non-SM underlying process.

Here we pursue another direction for discovery. We can utilize production and subsequent decays of other SUSY particles as a way to trigger on the events and learn more about the theory. For example, if sleptons or squarks are produced in a hadronic collision, they will cascade decay to high-p_T SM particles and charged and/or neutral Winos. The SM particles can be used for the trigger, and the cascade decays can be used to learn something about the spectroscopy of the theory.

Our example process is slepton and sneutrino production at the Tevatron which cascades into $l^+l^- + X_D$, where X_D is a displaced vertex from one or two $\tilde{W}^\pm \to \tilde{W}^0\pi^\pm$ decays. These displaced vertices are heavy charged particle tracks which stop in the vertex detector and produce very soft pions that may or may not be detectable. The dilepton events are produced through

$$p\bar{p} \to \tilde{\nu}_L\tilde{l}_L^\pm \;\; \to \;\; l^\pm l^\mp \tilde{W}^\pm\tilde{W}^0 \to l^\pm l^\mp + X_D + \not{E}_T \tag{29}$$

$$p\bar{p} \to \tilde{\nu}_L\tilde{\nu}_L \;\; \to \;\; l^\pm l^\mp \tilde{W}^\pm\tilde{W}^\mp \to l^\pm l^\mp + X_D + \not{E}_T\,. \tag{30}$$

In Fig. 4 we plot the total cross-section of such events for one flavor ($\mu^+\mu^- + X_D$) at the $\sqrt{s} = 2\,\text{TeV}$ Tevatron. We require the pseudo-rapidity to be within $|\eta| < 2$ for both leptons, and we require the leading lepton to have $p_T > 10\,\text{GeV}$, and the next lepton to have $p_T > 5\,\text{GeV}$. The total rate presented in Fig. 4 is calculated at leading order.

Our conclusion based on Fig. 4 is that left-handed sleptons with mass less than 185 GeV would be discovered at the Tevatron if $M_2 \lesssim m_{\tilde{\nu}_L} - 10\,\text{GeV}$ (for leptons to have high enough p_T for triggering) and if the Tevatron reaches at least 10 fb^{-1} integrated luminosity. This result is based on the requirement that more than 10 $l^+l^- + X_D$ events will occur for each flavor. We conservatively choose a 10 event requirement in order to ensure that our mass reach conclusion will remain valid if the dilepton identification efficiency were to be as low as 50% for the p_T acceptance cuts given above.

Other modes such as $\mu^\pm + X_D$ are possible in $\tilde{\nu}_L$ and $\tilde{\mu}_L$ production, and could confirm and extend the mass reach capabilities of the dilepton mode.

The dilepton signal discussed is essentially background free with the displaced vertices present [10]. However, the possibility of prompt Wino decays arises if μ is sufficiently light

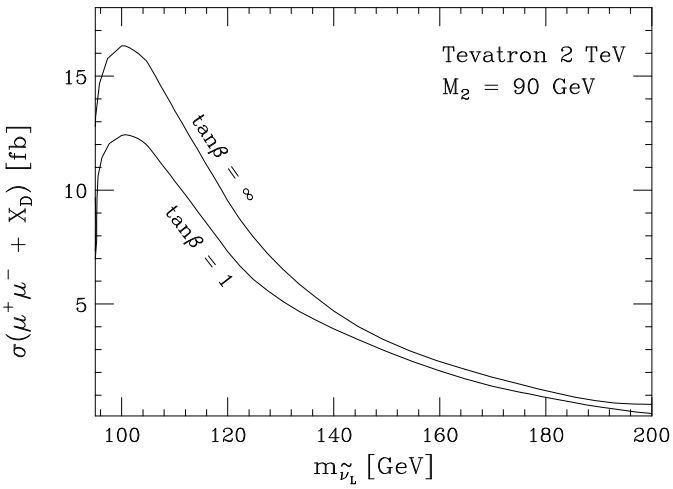

Figure 4: Dilepton signal with at least one displaced vertex from smuon and sneutrino production at the Fermilab Tevatron with 2 TeV center of mass energy and $M_2 = 90\,\mathrm{GeV}$. Acceptance cuts of the leptons and efficiencies are described in the text. The different curves are for $\tan\beta = 1$, which makes $m_{\tilde{\mu}_L} = m_{\tilde{\nu}_L}$, and for $\tan\beta = \infty$ which maximizes the hypercharge D-term splitting such that $m^2_{\tilde{\mu}_L} = m^2_{\tilde{\nu}_L} + m^2_W$. With 10 fb^{-1} the Tevatron will record more than 10 such events for each lepton flavor if $m_{\tilde{\nu}_L} < 185\,\mathrm{GeV}$.

to yield a chargino/neutralino mass splitting above 1 GeV. This would make the charged Wino decay promptly into a neutral Wino plus other states too soft to admit into the event description, and the resulting event would be difficult to separate from W^+W^- background. Also, if the top squarks are reduced from additional negative scalar mass sources, the mass splitting between the lightest chargino and neutralino could be greatly enhanced by loop corrections involving third family sfermions and fermions. In these cases, special triggers or analyses based on decay kinks of the charged Wino could not be relied upon, but the dilepton signal could remain useful with enough integrated luminosity. In addition to $\tilde{\nu}_L\tilde{\nu}_L$ and $\tilde{\nu}_L\tilde{l}$ production described above, the total dilepton sample also has contributions from $\tilde{l}_R\tilde{l}_R$ and $\tilde{l}_L\tilde{l}_L$ production that never yield dilepton signals plus a displaced vertex, and so were not counted before. Although the total rate of dilepton events increases by nearly a factor of two when we include $\tilde{l}_R\tilde{l}_R$ and $\tilde{l}_L\tilde{l}_L$ production, the lack of a displaced vertex makes it a challenge to separate it from SM backgrounds [13].

3.3 Degeneracy of sleptons

Another striking feature of the anomaly-mediated model with additional universal scalar terms is the near degeneracy of the left and right sleptons of the first two generations. The mass-squared splitting is somewhat insensitive to m_0,

$$\begin{aligned}\Delta_{\tilde{e}} &= m^2_{\tilde{e}_L} - m^2_{\tilde{e}_R} = (11\tan^4\theta_W - 1)\frac{3}{2}M_2^2 + \left(-\frac{1}{2} + 2\sin^2\theta_W\right) m_Z^2 \cos 2\beta \\ &\qquad + \frac{1}{8\pi^2}\left(\frac{9}{5}g_1^2 M_1^2 - 3g_2^2 M_2^2\right)\ln\frac{m_{\tilde{e}_R}}{m_Z} \\ &\simeq 0.037\left(-m_Z^2\cos 2\beta + M_2^2 \ln\frac{m_{\tilde{e}_R}}{m_Z}\right). \end{aligned} \tag{31}$$

The first term is the tree level anomaly-induced splitting, the second term is the hypercharge D-term splitting induced by electroweak breaking, and the third term is the one loop, leading log mass splitting induced by renormalizing the masses to their own scale. It is a numerical accident that the value of $\sin^2\theta_W$ is such that the M_2^2 coefficient in the first term of Eq. (31) is nearly zero. If,

$$\sin^2\theta_W = \frac{1}{1+\sqrt{11}} = 0.2317 \tag{32}$$

then the tree-level coefficient of M_2^2 would be identically zero. The actual value of $\sin^2\theta_W(m_Z)$ is 0.2312 ± 0.0003 [14] in the $\overline{MS}$ scheme and is extraordinarily close to the value in Eq. (32) required to make the M_2^2 coefficient in the tree-level mass splitting vanish.

It is also a numerical accident that the hypercharge D-term coefficient is suppressed since $\sin^2\theta_W \simeq 1/4$. Although the coefficient is not as spectacularly suppressed as the $m_{3/2}^2$ coefficient, it is multiplied by a fixed scale m_Z^2. Therefore, for a given value of $\tan\beta$ the mass squared difference remains constant regardless of how heavy the sleptons may be.

The degeneracy of the slepton can be characterized by the fractional difference,

$$\frac{m_{\tilde{e}_L} - m_{\tilde{e}_R}}{m_{\tilde{e}_R}} = -1 + \sqrt{1 + \frac{\Delta_{\tilde{e}}}{m^2_{\tilde{e}_R}}} \simeq \frac{1}{2}\frac{\Delta_{\tilde{e}}}{m^2_{\tilde{e}_R}}. \tag{33}$$

In Fig. 5 we plot contours of the relative mass splitting in the M_2-$m_{\tilde{e}_R}$ plane. The mass splitting is less than a few percent over most of parameter space. It exceeds 5% only when $M_2 > 350\,\mathrm{GeV}$. However, the squark masses in this case are over 2 TeV, which induces a considerable fine-tuning in the one-loop Higgs potential. Therefore, it is not expected that

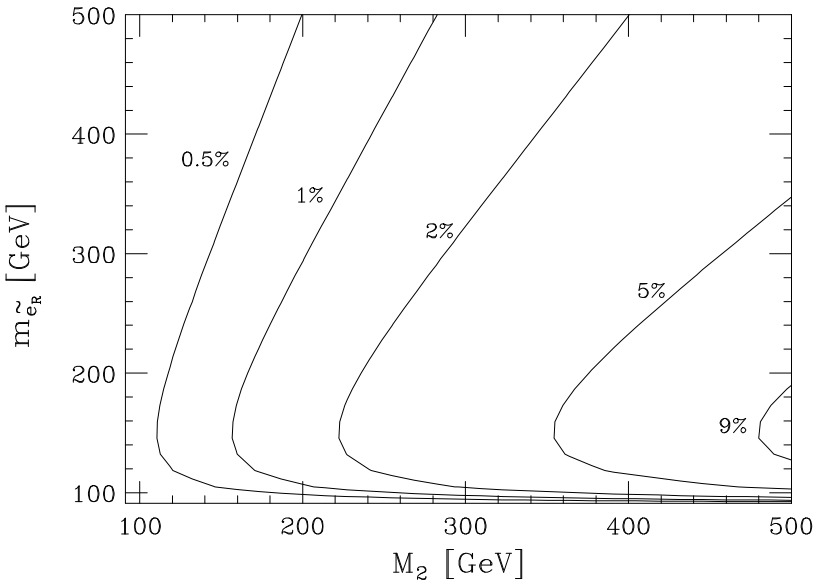

Figure 5: Contours of $100\% \times (m_{\tilde{e}_L} - m_{\tilde{e}_R})/m_{\tilde{e}_R}$ in the M_2-$m_{\tilde{e}_R}$ mass plane with large $\tan\beta$, which maximizes the mass splitting.

M_2 is so high, implying that the slepton mass differences should be no more than a few percent over the relevant parameter space.

The resolution of slepton masses from end-point lepton distributions of the slepton decays is approximately 2% at an e^+e^- or a muon collider [15]. Note that at a polarized linear collider it will not be difficult to determine that both left and right sleptons are being produced even if they are degenerate. This can be accomplished most effectively by comparing the total rate of slepton production with the asymmetry of production for polarized beams [15]. Degenerate sleptons are not expected in the usual supergravity or gauge-mediated scenarios, where $m_{\tilde{e}_R}$ is generally lighter than $m_{\tilde{e}_L}$. An exception to this is in the minimal supergravity model with $m_0 \gg m_{1/2}$. However, given the current limits on $m_{1/2}$ from gaugino searches at the Tevatron and LEP, degenerate sleptons will only occur at very high mass.

The above discussion is based on the assumption that the additional contributions to the slepton masses are universal. Since the anomaly-mediated mass differences is accidentally negligible, the degeneracy of the sleptons becomes a test of the additional mass contributions. Other approaches to the slepton tachyonic problem do not necessarily imply degenerate

slepton mass eigenstates [6].

3.4 LEP2 Signals

At LEP2 many signatures are possible in the AMSB scenario. The charged Winos have a large production cross section as long as they are kinematically accessible and as long as the sneutrino t-channel amplitude does not significantly interfere destructively with gauge boson s-channel amplitudes. Production of charginos at LEP has been the topic of many studies in supersymmetry phenomenology at LEP [16]. However, most of these studies have assumed that the LSP, the lightest neutralino, is more than a few GeV below the lightest chargino mass. In AMSB this is no longer the case. We expect that the lightest neutralino and charginos form a nearly degenerate $SU(2)$ triplet, as discussed in previous sections.

Since the chargino is only slightly above the neutralino in mass, the process $e^+e^- \to \tilde{W}^+\tilde{W}^-$ will be accompanied by very soft visible final states from decays such as $\tilde{W}^\pm \to \pi^\pm\tilde{W}^0$. These soft final states cannot be triggered on, which has led others [10, 12, 5] to suggest triggering on initial state photon radiation and then searching for soft, displaced tracks at the analysis level. However, there are other potential signatures of supersymmetry when Winos are the lightest gauginos. To enumerate them we must consider the other states in the supersymmetric spectrum which may be produced in collisions or as decay products of Wino production. In the AMSB scenario, the degenerate left and right sleptons and the sneutrino are the most important states at LEP after the gauginos. The ratio of their masses to the Wino masses is unknown in our framework, but it is more natural that they be somewhat light in order to keep the Higgs scalar potential from being fine-tuned. Therefore, considering phenomenological implications of light sleptons at LEP is useful.

There are many permutations to the relative ordering of M_2, $m_{\tilde{\nu}_L}$, and $m_{\tilde{e}} \equiv m_{\tilde{e}_{L,R}}$. Recall that the relationship between $m_{\tilde{e}}$ and $m_{\tilde{\nu}_L}$ is

$$m^2_{\tilde{e}_L} = m^2_{\tilde{\nu}_L} - m^2_W \cos 2\beta. \tag{34}$$

We can provide the general phenomenological features using a graph in the M_2-$m_{\tilde{\nu}_L}$ plane for LEP2 running at $\sqrt{s} = 200\,\mathrm{GeV}$. The results of the present and future experimental analyses combining the searches at LEP2 in different channels will be best presented as exclusion or

discovery regions in the M_2-$m_{\tilde{\nu}_L}$ plane. The LEP1 limit of Wino masses is slightly above $m_Z/2$, and the limit on sneutrino masses is slightly below $m_Z/2$; therefore, we begin the axes of Fig. 6 at $m_Z/2$. The lines represent kinematic boundaries. For example, the top dashed line is where $m_{\tilde{e}} = \sqrt{s}/2$, and for all $m_{\tilde{\nu}_L}$ values above that line, $\tilde{e}\tilde{e}$ production is not possible. The precise locations of the dashed lines depend on the choice of $\tan\beta$, which we choose to be $\tan\beta = 3$ for this figure.

Each region in the figure constitutes a different ordering of the mass eigenstates, and will produce a different set of useful observables with which to probe the theory. These observables are given inside the parentheses. For example, in the small triangular region surrounding the point $(M_2, m_{\tilde{\nu}_L}) = (95\,\mathrm{GeV}, 60\,\mathrm{GeV})$ one can search for $\gamma + \not{E}$, $l^+l^- + \not{E}$, and up to four electrons plus missing energy. Specific processes which lead to these signatures include,

$$e^+e^- \;\rightarrow\; \gamma\tilde{\nu}_L\tilde{\nu}_L \rightarrow \gamma + \not{E} \tag{35}$$

$$e^+e^- \;\rightarrow\; \tilde{W}^+\tilde{W}^- \rightarrow l^+l'^- + \not{E} \tag{36}$$

$$e^+e^- \;\rightarrow\; \tilde{l}^-\tilde{l}^+ \rightarrow l^+l^- + \not{E} \tag{37}$$

$$e^+e^- \;\rightarrow\; \tilde{W}^0\tilde{W}^0 \rightarrow \tilde{l}^+l^-\tilde{l}'^+l'^- \rightarrow l^+l^-l'^+l'^- + \not{E}. \tag{38}$$

Some of the leptons may be softer than others because of reduced phase space in a decay of a massive sparticle into a lepton and a sparticle with mass near its parent. Near the boundaries of the curves, it is often the case that some leptons are not energetic enough, and care must be taken in the analysis to identify them.

Finally, the stau sleptons may be lighter than the other sleptons, leading to more τ lepton final states than other leptons. Although efficiency in identifying τ leptons is smaller than the others, it is possible at large $\tan\beta$ to have large mixing among the $\tilde{\tau}_L$ and $\tilde{\tau}_R$ sleptons to produce a mass eigenstate accessible to LEP whereas the other sleptons are not.

4 Gravitino cosmology

A distinctive feature of the AMSB scenario is that the gravitino is much heavier than the supersymmetric partners of ordinary particles. The reason for this is that the AMSB masses

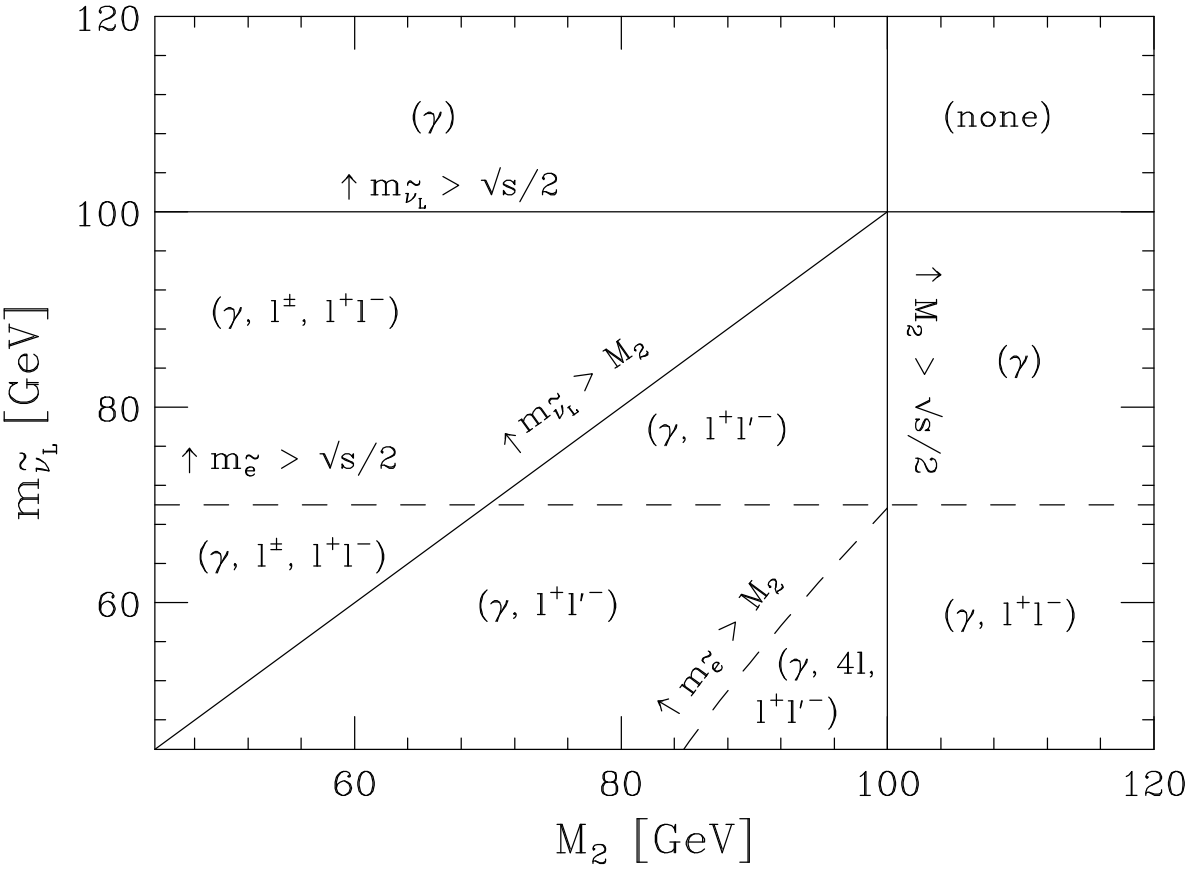

Figure 6: Signatures of the AMSB scenario at LEP2. Each blocked region has a unique mass hierarchy among $\tilde{\nu}_L$, $\tilde{e}_L$ and M_2, and therefore leads to different signatures which are contained within the parenthesis. The meaning of "(γ)", for example, is $e^+e^- \to \gamma\tilde{W}^+\tilde{W}^- \to \gamma + \not{E}$. We assume, as is justified by EWSB analysis, that M_2 is very close to the mass of the nearly degenerate lightest charginos and neutralino. The mass splitting between $m_{\tilde{\nu}_L}$ and $m_{\tilde{e}}$ is due to a hypercharge D-term, and its value is calculated with $\tan\beta = 3$ for this figure.

are suppressed by a loop factor relative to the gravitino mass $m_{3/2}$. In particular, one finds that the gravitino–Wino mass ratio is $m_{3/2}/M_2 \simeq 300$.

A large gravitino mass is cosmologically advantageous for solving the gravitino problem [17]. This problem occurs when gravitino decay products disrupt the light element abundance during nucleosynthesis. Even a period of inflation is not sufficient to solve this problem since gravitinos are thermally produced during the reheating phase of the universe [18]. Thus, in order for the gravitino decay products to be harmless during nucleosynthesis one either requires that the gravitino decays before affecting nucleosynthesis or that the reheating temperature of the universe be bounded from above.

The gravitino number density in units of the photon number density after the inflationary epoch is [19]

$$\frac{n_{3/2}}{n_\gamma}(T) = 2 \times 10^{-9} g_*(T)\ T_{13}(1 - 0.03 \ln T_{13}). \tag{39}$$

Here T_{13} is the reheating temperature after inflation in units of 10^{13} GeV (*i.e.*, $T_{13} \equiv T_R/10^{13}$ GeV), and $g_*(T)$ counts the massless degrees of freedom at the temperature T including a factor of 7/8 for fermions and the dilution factor for frozen-out species.

The gravitino decay width is

$$\Gamma_{3/2} = \frac{1}{4}\left(N_g + \frac{N_m}{12}\right)\frac{m_{3/2}^3}{M_P^2} \simeq 5.1\left(\frac{m_{3/2}}{50\ \text{TeV}}\right)^3 \text{sec}^{-1}. \tag{40}$$

Here $M_P = 1.2 \times 10^{19}$ GeV, N_g and N_m are the number of gauge and matter decay channels, and we have summed over all the SM particle content (N_g=12, N_m=49).

Immediately after the gravitino decays, the temperature of the universe is given by

$$T_D = \left(\frac{45\,\Gamma_{3/2}^2 M_P^2}{4\pi^3 g_*(T_D)}\right)^{1/4} = 2.7\left(\frac{10.75}{g_*(T_D)}\right)^{1/4}\left(\frac{m_{3/2}}{50\ \text{TeV}}\right)^{3/2} \text{MeV}. \tag{41}$$

Therefore for $m_{3/2} \lesssim 60$ TeV a detailed analysis of effects of gravitino decay during nucleosynthesis is necessary.

The particular gravitino decay products that cause the main interference during nucleosynthesis at early times ($\sim$ 1 second) are hadronic showers [20]. Photodissociations are not relevant at early stages of the nucleosynthesis epoch since the destructive photon-nucleus interactions are much less probable than photon-photon interactions. The overall

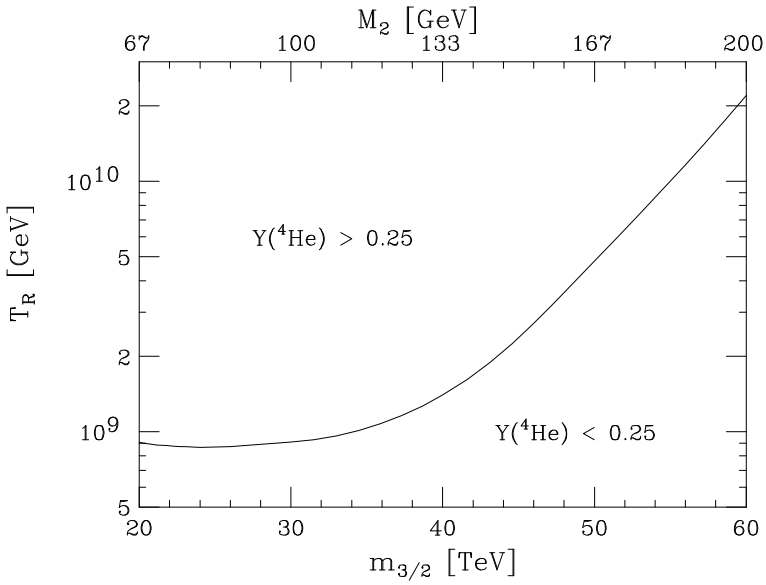

Figure 7: The upper bound on the reheat temperature as a function of the gravitino mass $m_{3/2}$ and the corresponding Wino mass M_2. The observational limit upper limit on the primordial helium abundance is $Y(^4\mathrm{He}) < 0.25$. Therefore, the region above the line is excluded, and an upper bound on T_R results.

effect of hadronic decay products is to convert protons into neutrons, and consequently the ^{4}He abundance is increased since the additional neutrons that are produced are synthesised into ^{4}He. Thus, using the observational upper limit on the primordial helium abundance $Y(^4\mathrm{He}) < 0.25$, we obtain an upper bound on the reheat temperature [21] which is depicted in Fig. 7. For $m_{3/2} \lesssim 40$ TeV, the typical bound on the reheat temperature is $T_R \sim 10^9$ GeV. This is typically less constraining than in the usual gravity-mediated scenarios with weak-scale gravitino mass [21].

As the gravitino mass increases, the upper bound on the reheat temperature becomes less significant, and completely evaporates for $m_{3/2} \gtrsim 60$ TeV, since the gravitinos decay well before the start of nucleosynthesis. For $m_{3/2} \gtrsim 60$ TeV, we may be concerned that the entropy produced by the gravitino decay excessively dilutes the baryon–to–photon ratio obtained by a primordial baryogenesis mechanism. However, this is never the case. Actually

for

$$\frac{m_{3/2}}{50\ \mathrm{TeV}} > 8\times 10^{-4}\left(\frac{g_*(T_D)}{10.75}\right)^{1/2} T_{13}^2(1-0.03\ln T_{13})^2, \tag{42}$$

the gravitino decays before dominating the universe and the entropy release is not dangerous. We have checked that, even when the gravitino matter-dominates the universe, the entropy production is not problematic. Therefore we conclude that when $m_{3/2} \gtrsim 60$ TeV, there is no upper bound on the reheat temperature arising from nucleosynthesis.

However, bounds on the reheating temperature when $m_{3/2} \gtrsim 60\,\mathrm{GeV}$ do come from considerations of the Wino energy density. The Wino thermal relic abundance Ω_{LSP}^{TH} does not play a significant cosmological role. Indeed Wino annihilations into gauge bosons in the early Universe are very efficient and lead to [4]

$$\Omega_{LSP}^{TH}h^2 \simeq 5\times 10^{-4}\left(\frac{M_2}{100\ \mathrm{GeV}}\right)^2. \tag{43}$$

On the other hand, a non-thermal production of LSPs is generated by the gravitino decay [22]. Since this decay occurs below the Wino freeze-out temperature, the LSP abundance is easily determined by assuming that each decaying gravitino produces a single Wino. The LSP is relativistic at decay time and becomes non-relativistic at a typical temperature $T \sim T_D M_2/m_{3/2}$, after red-shifting. The predicted relic abundance is

$$\Omega_{LSP}^{G}h^2 \simeq 30\left(\frac{M_2}{100\,\mathrm{GeV}}\right) T_{13}(1-0.03\ln T_{13}). \tag{44}$$

The requirement for not overclosing the universe leads to a bound on the reheat temperature $T_R \lesssim 10^{11}\,\mathrm{GeV}$. Of course, if R-parity is not conserved then this bound from LSP relic abundance is no longer relevant. In this case, for gravitino masses $m_{3/2} \gtrsim 60$ TeV, one can then contemplate using leptogenesis or even GUT baryogenesis mechanisms to generate the baryon asymmetry of the universe, consistently with the AMSB gravitino cosmology.

On the other hand, when $T_R \simeq 10^{10}$–$10^{11}\,\mathrm{GeV}$ the relic abundance of LSPs from gravitino decays is near critical density, providing a natural source of dark matter.

Finally, we comment on another positive aspect of the heavy gravitino cosmology. We can avoid the cosmological Polonyi problem that arises in the usual gravity-mediated scenario when the gauge singlet Polonyi field acquires a Planck scale vacuum expectation value but decays relatively late. In the AMSB scenario there is simply no need for the Polonyi field since the gaugino masses arise from a quantum anomaly.

5 Conclusion

In summary, anomaly-induced masses are always present when supersymmetry is broken. When these AMSB contributions dominate and yield all the gaugino masses as well as adding to universal scalar masses, a unique spectrum results which has important differences from other models of supersymmetry. Several of these unorthodox features that arise in low-energy supersymmetry from the AMSB scenario include,

- The ratio of gaugino masses $M_1 : M_2 : |M_3|$ is approximately $2.8 : 1 : 7.1$ when loop corrections are included, and $M_2 \simeq m_Z$;
- The lightest supersymmetric particle is most often the Wino, but may also be the sneutrino;
- Dilepton signals with displaced vertices are useful signals for this scenario at LEP and the Tevatron;
- The anomaly-induced contribution to left and right slepton masses is accidentally degenerate. This remains true if the required, additional sources for slepton masses are universal;
- LEP signatures are sensitive to the hierarchy of sneutrino, slepton and Wino masses. The searches in the different channels can be simply combined to give exclusion plots in the M_2-$m_{\tilde{\nu}_L}$ plane;
- The gravitino mass is much heavier than the masses of the other sparticles. Consequently, the cosmological problem associated with gravitino decays during nucleosynthesis is alleviated over much of parameter space;
- In spite of its negligible thermal relic abundance, neutral Winos can form the galactic dark matter, since they are copiously produced, below their freeze-out temperature, from the primordial gravitino decays.

Discovery of several of the above phenomenological implications is necessary to gain confidence that the AMSB scenario is a proper description of nature.

Appendix

Using Eqs. (12)-(14), the anomaly-mediated spectrum is

$$M_1 = \frac{33}{5}\frac{g_1^2}{16\pi^2}m_{3/2} \tag{45}$$

$$M_2 = \frac{g_2^2}{16\pi^2}m_{3/2} \tag{46}$$

$$M_3 = -3\frac{g_3^2}{16\pi^2}m_{3/2} \tag{47}$$

$$m^2_{\tilde{t}_R} = \left(-\frac{88}{25}g_1^4 + 8g_3^4 + 2y_t\hat{\beta}_{y_t}\right)\frac{m^2_{3/2}}{(16\pi^2)^2} \tag{48}$$

$$m^2_{\tilde{b}_R} = \left(-\frac{22}{25}g_1^4 + 8g_3^4 + 2y_b\hat{\beta}_{y_b}\right)\frac{m^2_{3/2}}{(16\pi^2)^2} \tag{49}$$

$$m^2_{\tilde{Q}_3} = \left(-\frac{11}{50}g_1^4 - \frac{3}{2}g_2^4 + 8g_3^4 + y_t\hat{\beta}_{y_t} + y_b\hat{\beta}_{y_b}\right)\frac{m^2_{3/2}}{(16\pi^2)^2} \tag{50}$$

$$m^2_{H_u} = \left(-\frac{99}{50}g_1^4 - \frac{3}{2}g_2^4 + 3y_t\hat{\beta}_{y_t}\right)\frac{m^2_{3/2}}{(16\pi^2)^2} \tag{51}$$

$$m^2_{H_d} = \left(-\frac{99}{50}g_1^4 - \frac{3}{2}g_2^4 + 3y_b\hat{\beta}_{y_b} + y_\tau\hat{\beta}_{y_\tau}\right)\frac{m^2_{3/2}}{(16\pi^2)^2} \tag{52}$$

$$m^2_{\tilde{L}_3} = \left(-\frac{99}{50}g_1^4 - \frac{3}{2}g_2^4 + y_\tau\hat{\beta}_{y_\tau}\right)\frac{m^2_{3/2}}{(16\pi^2)^2} \tag{53}$$

$$m^2_{\tilde{\tau}_R} = \left(-\frac{198}{25}g_1^4 + 2y_\tau\hat{\beta}_{y_\tau}\right)\frac{m^2_{3/2}}{(16\pi^2)^2} \tag{54}$$

$$A_{y_t} = -\frac{\hat{\beta}_{y_t}}{y_t}\frac{m_{3/2}}{16\pi^2} \tag{55}$$

$$A_{y_b} = -\frac{\hat{\beta}_{y_b}}{y_b}\frac{m_{3/2}}{16\pi^2} \tag{56}$$

$$A_{y_\tau} = -\frac{\hat{\beta}_{y_\tau}}{y_\tau}\frac{m_{3/2}}{16\pi^2}. \tag{57}$$

where

$$\hat{\beta}_{y_t} = 16\pi^2\beta_{y_t} = y_t\left(-\frac{13}{15}g_1^2 - 3g_2^2 - \frac{16}{3}g_3^2 + 6y_t^2 + y_b^2\right) \tag{58}$$

$$\hat{\beta}_{y_b} = 16\pi^2\beta_{y_b} = y_b\left(-\frac{7}{15}g_1^2 - 3g_2^2 - \frac{16}{3}g_3^2 + y_t^2 + 6y_b^2 + y_\tau^2\right) \tag{59}$$

$$\hat{\beta}_{y_\tau} \;=\; 16\pi^2\beta_{y_\tau} = y_\tau\left(-\frac{9}{5}g_1^2 - 3g_2^2 + 3y_b^2 + 4y_\tau^2\right). \tag{60}$$

The first two generation squark and slepton masses are obtained by appropriately changing the Yukawa couplings to first and second generation Yukawa couplings.

References

[1] A.H. Chamseddine, R. Arnowitt, and P. Nath, Phys. Rev. Lett. **49**, 970 (1982);
R. Barbieri, S. Ferrara, and C.A. Savoy, Phys. Lett. B **119**, 343 (1982);
for a review, see H.P. Nilles, Phys. Rep. **110**, 1 (1984).

[2] M. Dine and A.E. Nelson, Phys. Rev. D **48**, 1277 (1993);
M. Dine, A.E. Nelson, and Y. Shirman, Phys. Rev. D **51**, 1362 (1995);
M. Dine, A.E. Nelson, Y. Nir, and Y. Shirman, Phys. Rev. D **53**, 2658 (1996);
for a review, see G.F. Giudice and R. Rattazzi, hep-ph/9801271.

[3] L. Randall and R. Sundrum, hep-th/9810155.

[4] G.F. Giudice, M.A. Luty, H. Murayama, and R. Rattazzi, hep-ph/9810442.

[5] J.L. Feng, T. Moroi, L. Randall, M. Strassler, and S. Su, hep-ph/9904250.

[6] A. Pomarol and R. Rattazzi, hep-ph/9903448.

[7] G.F. Giudice and A. Masiero, Phys. Lett. B **206**, 480 (1988).

[8] G.F. Giudice and R. Rattazzi, Nucl. Phys. B **511**, 25 (1998);
N. Arkani-Hamed, G.F. Giudice, M.A. Luty, and R. Rattazzi, Phys. Rev. D **58**, 115005 (1998).

[9] D.M. Pierce, J.A. Bagger, K. Matchev, and R.-J. Zhang, Nucl. Phys. B **491**, 3 (1997).

[10] C.H. Chen, M. Drees, and J.F. Gunion, Phys. Rev. Lett. **76**, 2002 (1996), Phys. Rev. D **55**, 330 (1997), addendum/erratum in hep-ph/9902309.

[11] H.-C. Cheng, B.A. Dobrescu, K.T. Matchev, Nucl. Phys. B **543**, 47 (1999).

[12] S. Thomas and J.D. Wells, Phys. Rev. Lett. **81**, 34 (1998).

[13] H. Baer, C.-h. Chen, C. Kao, and X. Tata, Phys. Rev. D **52**, 1565 (1995); H. Baer, C.-h. Chen, F. Paige, and X. Tata, Phys. Rev. D **54**, 5866 (1996).

[14] Particle Data Group (C. Caso *et al.*), *Review of Particle Physics*, Eur. Phys. J. C **3**, 1 (1998).

[15] M. Danielson *et al.*, "Supersymmetry at the NLC," Proceedings of the Workshop on Future Directions in High Energy Physics (Snowmass 1996);
B. Autin, A. Blondel, J. Ellis, *et al.*, "Prospective Study of Muon Storage Rings at CERN", CERN preprint 1999.

[16] G. Altarelli *et al.*, "Searches for New Physics", in Physics at LEP, hep-ph/9602207.

[17] S. Weinberg, Phys. Rev. Lett. **48**, 1303 (1982).

[18] J. Ellis, J.E Kim and D.V Nanopoulos, Phys. Lett. B **145**, 181 (1984)

[19] M. Kawasaki and T. Moroi, Prog. Theor. Phys. **93**, 879 (1995).

[20] M.H. Reno and D. Seckel, Phys. Rev. D **37**, 3441 (1988).

[21] See, for example, S. Sarkar, Rept. Prog. Phys. **59**, 1493 (1996).

[22] J.A. Frieman and G.F. Giudice, Phys. Lett. B **224**, 125 (1989)